UDK 66.040:691.714.018.8:621.785.6
Original scientific article/Izvirni znanstveni članek

ISSN 1580-2949
MTAEC9, 55(2)243(2021)

MODIFIED PHYSICALLY-BASED CONSTITUTIVE MODEL FOR As-CAST Mn18Cr18N AUSTENITIC STAINLESS STEEL AT ELEVATED TEMPERATURES

MODIFICIRAN FIZIKALNI KONSTITUTIVNI MODEL VROČE DEFORMACIJE LITEGA AVSTENITNEGA NERJAVNEGA JEKLA VRSTE Mn18Cr18N

Jihong Tian, Fei Chen, Fengming Qin, Jiansheng Liu, Huiqin Chen*

School of Materials Science and Engineering, Taiyuan University of Science and Technology, Taiyuan 030024, P. R. China

Prejem rokopisa – received: 2020-08-23; sprejem za objavo – accepted for publication: 2020-11-12

doi:10.17222/mit.2020.168

The hot-deformation behavior of the as-cast Mn18Cr18N high-nitrogen austenitic stainless steel, produced with the electroslag-remelting metallurgical technology, was studied using isothermal-compression tests in a temperature range of 1223–1473 K) and a strain-rate range of 0.001–1 s^{-1}). The flow-stress curves of the Mn18Cr18N steel were obtained under different hot-deformation conditions. By establishing the hyperbolic sine-law Zener-Hollomon equation, the hot-deformation activation energy of the Mn18Cr18N steel was obtained. Based on the mechanism of dislocation evolution, a physically-based constitutive model was established. In addition, the expression of the dynamic-recovery coefficient of the model was modified. Compared with the model before the modification, the modified constitutive model could effectively improve the prediction accuracy of the flow stress for the as-cast Mn18Cr18N austenitic stainless steel.

Keywords: as-cast Mn18Cr18N, work hardening, dynamic recovery, dynamic recrystallization, constitutive model

Avtorji v članku opisujejo študijo vroče deformacije litega Mn18Cr18N nerjavnega jekla z visoko vsebnostjo dušika. Jeklo je bilo izdelano s postopkom elektro-pretaljevanja pod žlindro. Preizkuse so izvajali s tlačno deformacijo v temperaturnem območju med 1223 K in 1473 K ter pri hitrostih deformacije med 0,001 s^{-1} in 1 s^{-1}. Izdelali so krivulje tečenja izbranega jekla pri različnih pogojih vroče deformacije. Po potrditvi sinus-hiperboličnega zakona Zener–Hollomon enačbe, so določili še aktivacijsko energijo za vročo deformacijo jekla Mn18Cr18N. Na osnovi mehanizma razvoja dislokacij so izdelali fizikalni konstitucijski model. Dodatno so modificirali izraz za koeficient poprave v modelu. Primerjava modelov, brez in z modifikacijo, je pokazala, da modificirani konstitutivni model lahko učinkoviteje izboljša natančnost napovedi poteka krivulj tečenja izbranega litega avstenitnega jekla vrste Mn18Cr18N.

Ključne besede: lito avstenitno jeklo Mn18Cr18N, deformacijsko utrjevanje, dinamična poprava, dinamična rekristalizacija, konstitutivni model

1 INTRODUCTION

The development of the ultra-supercritical-unit manufacturing technology is an important way of realizing energy conservation and emission reduction while developing the basic industry. The Mn18Cr18N stainless steel is used in the generator ring, which is one of the important basic parts of an ultra-supercritical unit due to its excellent corrosion resistance, ductility and toughness.[1–3] The forming of a generator ring usually includes ingot cogging, punching and bulging. In the forging process, the processing is various and the process is complex. However, there are a few researches on the plastic-deformation behavior of the as-cast Mn18Cr18N austenitic stainless steel using the electroslag-remelting (ESR) process at an elevated temperature. The rheological behavior of a metal at an elevated temperature is closely related to the strain, strain rate and deformation temperature.[4] Based on the coupling of work hardening and dynamic softening during deformation, flow-stress curves tend to exhibit a highly nonlinear law.[5] Therefore, a study of the thermal-deformation behavior of the as-cast ESR Mn18Cr18N at an elevated temperature and establishment of a high-precision nonlinear constitutive model are important for the optimization of the production processes and quality improvement of the generator ring.

A lot of research on the hot-deformation behavior of metals has done by many scholars. J. H. Hollomon[6] proposed a flow-stress model, which took into account that the flow stress was an exponential function of strain. C. M. Sellars et al.[7,8] proposed a hyperbolic-sine mathematical model to characterize the flow stress of a metal. B. S. Yu et al.[9] systematically studied the stress-strain curves of a shape-memory alloy (SMA), using a neural-network algorithm with back-propagation training to establish a nonlinear model based on the experimental results for the SMA. L. Li et al.[10] analyzed the hot-deformation dynamics and flow stability of a TC17 alloy, and a strain-compensated constitutive model of the TC17 alloy was established.[10] A modified steel J-C model for 10%Cr was

*Corresponding author's e-mail:
chen_huiqin@126.com (Huiqin Chen)

Table 1: Chemical composition of the as-cast Mn18Cr18N austenitic stainless steel (*w*/%)

Cr	Mn	N	Ni	Mo	Cu	Si	Al	C	Ti	P	S
20	19.21	0.61	0.14	0.022	0.035	0.59	0.023	0.074	0.016	0.014	0.001

developed by J. L. He et al.[11] on the basis of the traditional J-C constitutive model. This modified model not only considered the coupling effects of the strain, strain rate and temperature, but also introduced work hardening and dynamic softening into the entire deformation to improve the accuracy of the traditional J-C constitutive model. Based on the stress-dislocation relationship and dynamic recrystallization dynamics, a two-stage constitutive model was established to predict the flow stress of nickel-based superalloys by Y .C. Lin et al.[12] G. Z. Voyiadjis et al.[13] developed a physically-based constitutive model to describe the high-temperature deformation behavior of face-centered cubic metals. The expression of the flow stress was used to simulate the experimental results of oxygen-free high-conductivity copper at different temperatures and strain rates. F. Chen et al.[14] using isothermal-compression tests obtained the flow-stress curves of the as-cast CL70 steel. To forecast the flow stress for forging, a constitutive model based on the dislocation-density evolution was established.

Constitutive models have been studied for over a hundred years and researchers have constructed various constitutive models using different methods. Among these models, the physically-based constitutive model based on the dislocation-evolution mechanism is one of the most accurate constitutive models. In view of the fact that the studies on the constitutive model of the as-cast Mn18Cr18N steel produced with electroslag remelting are relatively rare at present, this paper obtained the flow-stress curves of the as-cast Mn18Cr18N steel based on isothermal-compression test, established a physically-based constitutive model and modified the model to improve its accuracy. This provides a reference for the optimization of the cogging process for the as-cast Mn18Cr18N.

2 EXPERIMENTAL PART

The experimental material used in this paper is the as-cast Mn18Cr18N austenitic stainless steel received as an ingot cast with electroslag remelting. Its specific chemical composition is shown in **Table 1**. An isothermal-compression test was used to investigate the elevated-temperature deformation behavior of the steel. The experiment was carried out on a Thermecmastor-Z thermal mechanical simulator.

A standard sample for a compression test is a (Φ8×12) mm cylinder. And the specimen should be heated to 1473 K and kept warm for 120 s. Then, it should be cooled to the deformation temperature and kept warm for 60 s. The deformation was 50 %. The deformation temperature was 1223–1473 K and the strain rate was 0.001–1 s^{-1}. Finally, the hot-deformation sample was cooled to room temperature with liquid nitrogen at a cooling rate of 50 K/s.

3 RESULTS AND DISCUSSION

3.1 Characteristics of the flow stress

Figure 1 shows the flow-stress curves of the as-cast Mn18Cr18N steel. As shown, the Mn18Cr18N steel has two types of stress-strain curves, representing work hardening/dynamic recovery and dynamic recrystallization.

A work hardening/dynamic recovery curve is expressed in two different stages with an increase in the strain at a high temperature. In the first stage, the flow stress increases with the increase in the strain, while the growth rate decreases gradually. This is because the increase of dislocations caused by work hardening (WH) is greater than the loss of dislocations caused by dynamic recovery (DRV), resulting in an increased stress. In the second stage, the flow stress is in a relatively stable state.

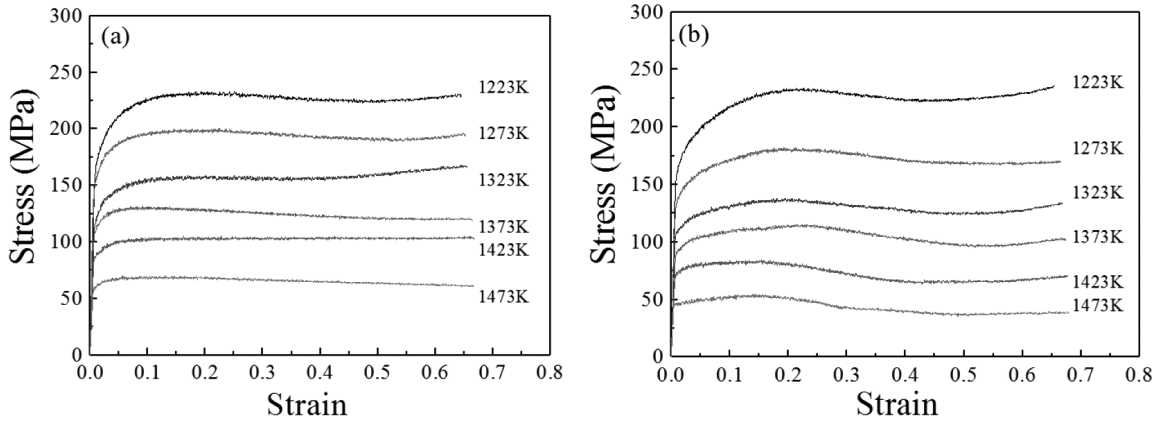

Figure 1: Flow-stress curves of the as-cast Mn18Cr18N steel: a) the strain rate of 1 s^{-1}, b) the strain rate of 0.1 s^{-1}

At this point, the dislocation increment caused by WH is equivalent to the dislocation disappearance caused by DRV, and the stress does not increase any more.

The dynamic-recrystallization (DRX) curve is divided into three stages. At the beginning, WH is dominant and the flow stress increases to the critical stress of DRX. Then, the flow stress reaches the peak and begins to fall until the curve stabilizes, as DRV and DRX play a significant softening role in this phase. However, the hardening effect is still greater than the softening effect. In the third stage, as the DRX softening increases, the flow stress decreases. Finally, due to the same degree of hardening and softening, the dislocation annihilation rate is equal to the dislocation proliferation rate, and the flow-stress curve tends to be stable.

3.2 Arrhenius model

Based on the thermal-mechanical coupling, C. M. Sellars and W. J. Tegart proposed the following models:[7,8]

$$\dot{\varepsilon} = \begin{cases} A[\sinh(\alpha\sigma)]^n \exp\left(-\dfrac{Q}{RT}\right) \\ A'\sigma^{n'}(\alpha\sigma < 0.8) \\ A''\exp(\beta\sigma)(\alpha\sigma > 1.2) \end{cases} \quad (1)$$

Then, Equation (2) can be obtained with a logarithmic transformation of Equation (1):

$$\ln\dot{\varepsilon} = \begin{cases} n\ln[\sinh(\alpha\sigma)] + \ln A - \dfrac{Q}{RT} \\ n'\ln\sigma + \ln A' \\ \beta\sigma + \ln A' \end{cases} \quad (2)$$

According to the isothermal-compression experiment, the peak stresses of the Mn18Cr18N austenitic stainless steel can be obtained from the stress-strain curves under different deformation conditions. The relational graphs for ln $\dot{\varepsilon}$ and ln σ_p, σ_p are established, as shown in **Figures 2a** and **2b**. The slopes can be determined with linear fitting. So, $n' = 9.136$, $\beta = 0.0845$ and coefficient $\alpha = \beta/n' = 0.00925$. Based on Equation (2), the relational graphs between $\ln[\sinh(\alpha\sigma_p)]$ and ln $\dot{\varepsilon}$, $1000/T$, are established, as shown in **Figures 2c** and **2d**. Using the same method, it can be found that $n = 6.768$, $Q/1000nR = 12.637$ and $A = 7.067 \times 10^{25}$. Finally, the activation energy of hot deformation of the as-cast Mn18Cr18N steel was obtained, $Q = 711073.274$ J/mol.

To make it easier to characterize the effects of the strain, strain rate and deformation temperature on the flow stress, Zener and Hollomon introduced the Zener-Hollomon parameter, represented by letter Z.[15] The expression of parameter Z is shown in Equation (3):

$$Z = \dot{\varepsilon}\exp\left(\frac{Q}{RT}\right) \quad (3)$$

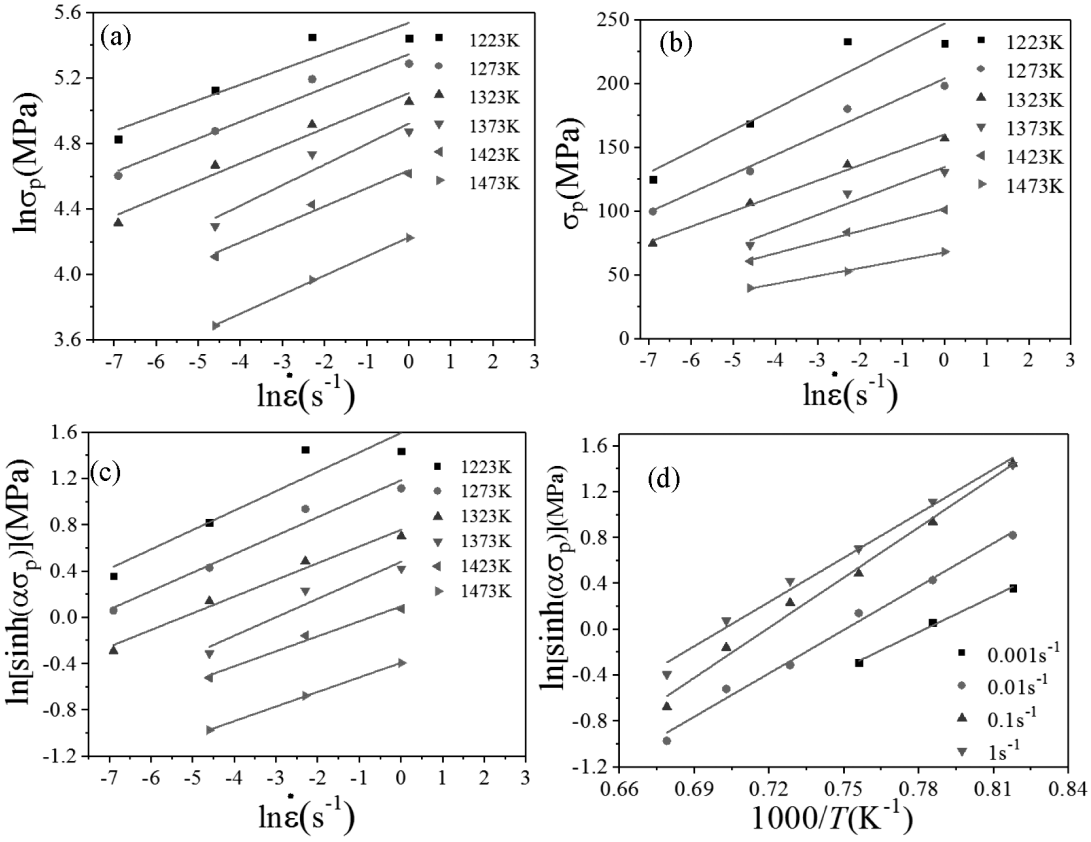

Figure 2: Relationship between σ_p and $\dot{\varepsilon}$, T: a) ln σ_p – ln $\dot{\varepsilon}$, b) σ_p – ln $\dot{\varepsilon}$, c) $\ln[\sinh(\alpha\sigma_p)]$ – ln $\dot{\varepsilon}$, d) $\ln[\sinh(\alpha\sigma_p)]$ – $1000/T$

According to the above calculation results, parameter Z can be expressed as follows:

$$Z = \dot{\varepsilon} \exp\left(\frac{711073.274}{RT}\right) = \\ = 7.067 \times 10^{25} \left[\sinh(0.00925\sigma_p)\right]^{6.768} \quad (4)$$

Equation (4) can be rewritten to calculate the peak stress:

$$\sigma_p = 4108.11 \sinh^{-1}(000152Z^{0.1478}) \quad (5)$$

3.3 Work hardening/dynamic recovery modelling

According to WH and DRV, the evolution of the dislocation density with strain can be expressed as:[16]

$$\frac{d\rho}{d\varepsilon} = k_1\sqrt{\rho} - k_2\rho \quad (6)$$

where $d\rho/d\varepsilon$ is the increasing rate of the dislocation density with strain, ρ is the dislocation density, k_1 is the work-hardening coefficient and k_2 is the dynamic-recovery coefficient. During the hot-deformation process, the evolution law for the flow stress of the material with the dislocation density is expressed as:[17,18]

$$\sigma_{rec} = \alpha\mu b\sqrt{\rho} \quad (7)$$

where α is the material constant, μ is the shear modulus and b is the Burgers vector.

By taking a derivative of Equation (7) with respect to ρ, Equation (8) can be obtained:

$$\frac{d\sigma_{rec}}{d\rho} = \frac{\alpha\mu b}{2\sqrt{\rho}} \quad (8)$$

Synthesizing Equations (6) and (8), the work-hardening rate θ can be expressed with the following formula:

$$\theta = \frac{d\sigma_{rec}}{d\varepsilon} = \frac{d\sigma}{d\varepsilon}\cdot\frac{d\sigma_{rec}}{d\rho} = \\ = \frac{\alpha\mu b k_1 - \alpha\mu b k_2\sqrt{\rho}}{2} = \frac{\alpha\mu b k_1 - k_2\sigma_{rec}}{2} \quad (9)$$

When $\theta = 0$, σ_{sat} is shown as:

$$\sigma_{sat} = \frac{\alpha\mu b k_1}{k_2} \quad (10)$$

where σ_{sat} is the saturated stress. Based on Equation (9), $d\varepsilon$ is readily expressed with the equivalent transformation as:

$$d\varepsilon = \frac{d\sigma_{rec}}{\theta} = \frac{2d\sigma_{rec}}{\alpha\mu b k_1 - k_2\sigma_{rec}} \quad (11)$$

Integrating Equation (11), Equation (12) is obtained:

$$\varepsilon = -\frac{2}{k_2}\ln(\alpha\mu b k_1 - k_2\sigma_{rec}) + C_1 \quad (12)$$

Then, Equation (12) can be written as:

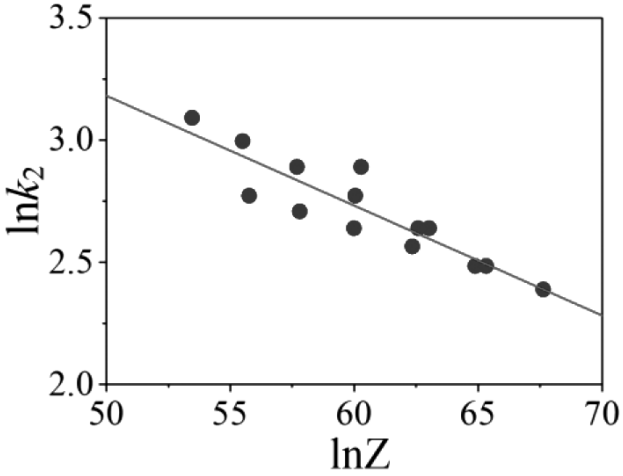

Figure 3: Relationship between k_2 and ln Z

$$\alpha\mu b k_1 - k_2\sigma_{rec} = C_2 \exp\left(-\frac{k_2}{2}\varepsilon\right) \quad (13)$$

For $\varepsilon = 0$ and $\sigma = \sigma_0$, Equation (13) is written as:

$$C_2 = \alpha\mu b k_1 - k_2\sigma_0 \quad (14)$$

where σ_0 is the yield stress.

Synthesizing Equations (13) and (14), the flow stress is written as Equation (15):

$$\sigma_{rec} = \frac{\alpha\mu b k_1 - (\alpha\mu b k_1 - k_2\sigma_0)\exp\left(-\frac{k_2}{2}\varepsilon\right)}{k_2} = \\ = \sigma_{sat} - (\sigma_{sat} - \sigma_0)\exp\left(-\frac{k_2}{2}\varepsilon\right) \quad (15)$$

And yield stress σ_0 can be written as a function of peak stress. Using linear fitting, the yield stress can be expressed as Equation (16):

$$\sigma_0 = 0.681\sigma_p + 14.636 \quad (16)$$

In addition, dynamic-recovery coefficient k_2 can be obtained with Equation (15). According to **Figure 3**, coefficient k_2 can be expressed as:

$$k_2 = 228.0238Z^{-0.04496} \quad (17)$$

Besides, the saturated stress can be expressed as a function of peak stress. Using linear fitting, the saturated stress can be expressed with Equation (18):

$$\sigma_{sat} = 0.998\sigma_p + 2.823 \quad (18)$$

In short, the constitutive model for the as-cast Mn18Cr18N during the work hardening/dynamic recovery stage can be written as:

$$\begin{cases} \sigma_{rec} = \sigma_{sat} - (\sigma_{sat} - \sigma_0)\exp(-k_2\varepsilon/2) \\ \sigma_{sat} = 0.998\sigma_p + 2.823 \\ \sigma_0 = 0.681\sigma_p + 14.636 \\ k_2 = 228.0238Z^{-0.04496} \\ Z = \dot{\varepsilon}\exp(711073.274/RT) \\ \sigma_p = 108.11\sinh^{-1}(0.000152Z^{0.1478}) \end{cases} \quad (19)$$

3.4 Dynamic-recrystallization modelling

When plastic deformation occurs at a higher temperature or lower strain rate, DRX starts when the strain reaches a certain threshold. The volume-fraction model of DRX can be described with the following formula:[19,20]

$$X_d = 1 - \exp\left[-k_d\left(\frac{\varepsilon - \varepsilon_c}{\varepsilon_p}\right)^{n_d}\right] \quad (20)$$

where k_d, n_d are the material constants. And the volume fraction of DRX can also be calculated as Equation (21):

$$X_d = \frac{\sigma_{rec} - \sigma}{\sigma_{sat} - \sigma_{ss}} \quad (21)$$

Combining Equations (20) and (21), the flow stress can be written as:

$$\sigma = \sigma_{WH} - (\sigma_{sat} - \sigma_{ss})\left\{1 - \exp\left[-k_d\left(\frac{\varepsilon - \varepsilon_c}{\varepsilon_p}\right)^{n_d}\right]\right\}(\varepsilon \geq \varepsilon_c) \quad (22)$$

The steady-state stress can also be expressed as a function of peak stress. Using linear fitting, the steady-state stress can be expressed with Equation (23):

$$\sigma_{ss} = 1.006\sigma_p - 14.720 \quad (23)$$

The peak stress is an important characteristic point of the flow-stress curve, which indicates that the increment and decrease of dislocations in the metal are equal for the first time, after which the stress begins to decrease. The strain corresponding to the peak stress is the peak strain, which can be expressed with the following formula:

$$\varepsilon_p = C_3 Z^{k_3} \quad (24)$$

After the transformation, Equation (24) is expressed as:

$$\ln\varepsilon_p = \ln C_3 + k_3 \ln Z \quad (25)$$

Figure 4 shows the relationship between ln ε_p and ln Z. Using linear fitting, it can be found that k_3 = 0.10705 and $C_3 = 1.11\times10^{-4}$. Then, Equation (24) is rewritten as:

$$\varepsilon_p = 1.11\times10^{-4} Z^{0.10705} \quad (26)$$

One of the important parameters of a metal constitutive model is the critical strain, which represents the starting point of dynamic recrystallization. It is generally assumed that the critical strain ε_c = 0.6–0.85. Since this parameter is difficult to obtain accurately, based on the previous research results, it is determined that $\varepsilon_c = 0.8\varepsilon_p$.[20] Then it can be written as Equation (27):

$$\varepsilon_c = 0.8\varepsilon_p \quad (27)$$

After the transformation, Equation (20) is expressed as:

$$\ln[-\ln(1-X_d)] = \ln k_d + n_d \ln\left(\frac{\varepsilon - \varepsilon_c}{\varepsilon_p}\right) \quad (28)$$

Figure 5 shows the relationship between ln[-ln(1-X_d)] and ln[(ε-ε_c)/ε_p]. Using linear fitting, coefficients k_d and n_d are 0.02324 and 2.343, respectively.

According to the above calculation results, the volume-fraction model of DRX can be expressed as:

$$X_d = 1 - \exp\left[\left(\frac{\varepsilon - 0.8\varepsilon_p}{\varepsilon_p}\right)^{2.343}\right] \quad (29)$$

In conclusion, the dynamic-recrystallization constitutive model for the as-cast Mn18Cr18N steel can be written as:

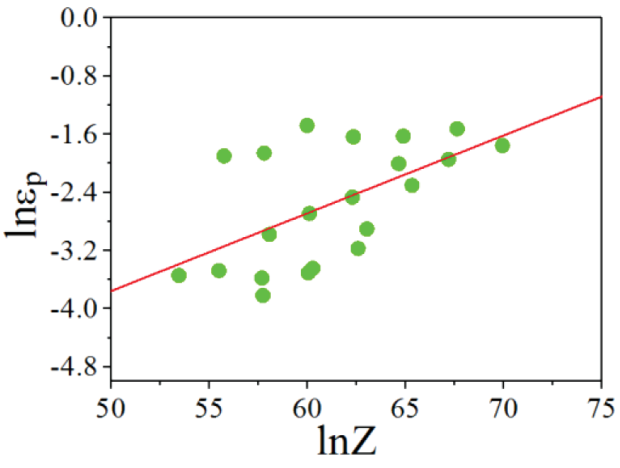

Figure 4: Relationship between ln ε_p and ln Z

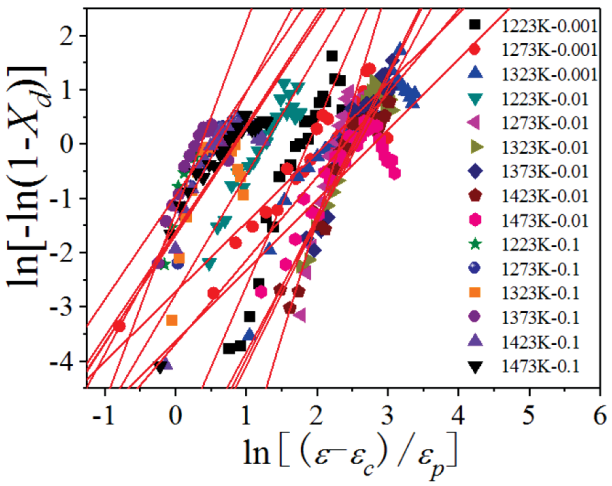

Figure 5: Relationship between ln [–ln(1–X_d)] and ln[(ε-ε_c)/ε_p]

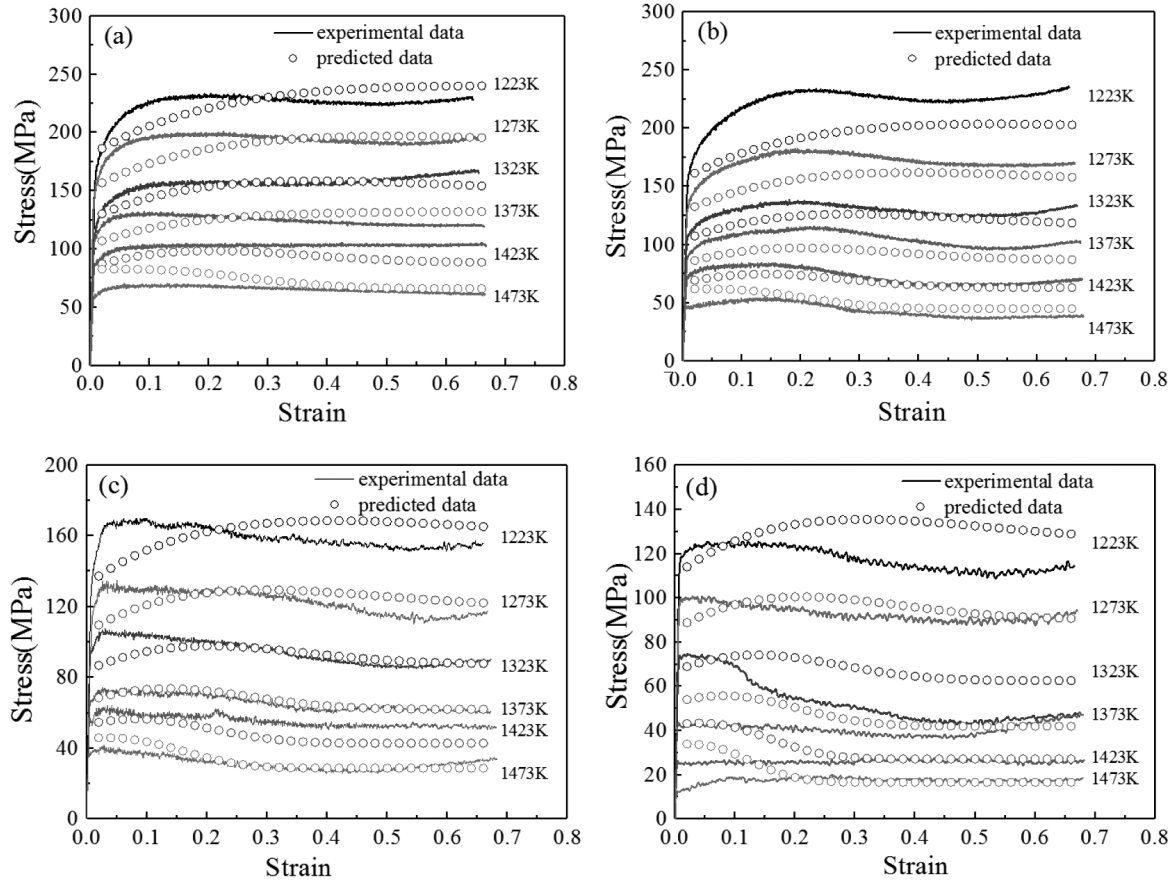

Figure 6: Comparison between the experimental and predicted flow stress at different strains for strain rates of a) 1 s^{-1}, b) 0.1 s^{-1}, c) 0.01 s^{-1}, d) 0.001 s^{-1}

$$\begin{cases} \sigma_{rec} = \sigma_{rec} - (\sigma_{sat} - \sigma_0)\left\{1 - \exp\left[-0.02324\left(\dfrac{\varepsilon - \varepsilon_c}{\varepsilon_p}\right)^{2.343}\right]\right\} (\varepsilon \geq \varepsilon_c) \\ \sigma_{rec} = \sigma_{rec} - (\sigma_{sat} - \sigma_{ss})\exp(-k_2\varepsilon/2) \\ \sigma_{sat} = 0.998\sigma_p + 2.823 \\ \sigma_{ss} = 1.006\sigma_p - 14.720 \\ \sigma_0 = 0.681\sigma_p + 14.636 \\ \sigma_p = 108.11\sinh^{-1}(0.000152Z^{0.1478}) \\ k_2 = 228.0238Z^{-0.04496} \\ Z = \dot{\varepsilon}\exp(711073.274/RT) \\ \varepsilon_p = 1.11\times10^{-4}Z^{0.10705} \\ \varepsilon_c = 0.88\times10^{-5}Z^{0.10705} \end{cases} \quad (30)$$

3.5 Model validation

According to the calculation above, the constitutive model of the as-cast Mn18Cr18N steel was obtained. In this paper, the mean absolute relative error (AARE) and root mean square error (RMSE) of the constitutive model were calculated based on Equations (31) and (32) to obtain the reliability and accuracy of the model:

$$AARE = \frac{1}{n}\sum_{i=1}^{n}\left|\frac{\sigma_e - \sigma_p}{\sigma_e}\right| \times 100\ \% \quad (31)$$

$$RMSE = \sqrt{\frac{1}{n}\sum_{i=1}^{n}(\sigma_e - \sigma_p)^2} \quad (32)$$

where σ_e is the measured flow stress, σ_p is the flow stress predicted by the constitutive model and n is the total number of data sets, used to verify the model.

Figure 6 shows graphs of comparisons of the constitutive model and experiments. The results show that the AARE is 14.9 % and the RMSE is 21.1 MPa.

3.6 Model modification

This physically-based constitutive model includes the values of flow stress for a higher accuracy of prediction. However, in the process of establishing the model, dynamic-recovery coefficient k_2 depends on the Z parameter, which is related to the deformation temperature and strain rate. When ignoring the effect of strain on dynamic-response coefficient k_2, it is easy to create a model at the starting point of the deformation-rheological stress, which increases the error of the predicted value. In order to improve the accuracy of the model, the effect

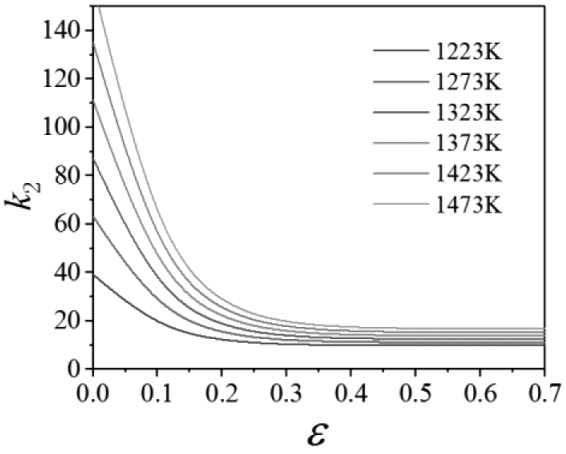

Figure 7: Relationship between k_2 and strain

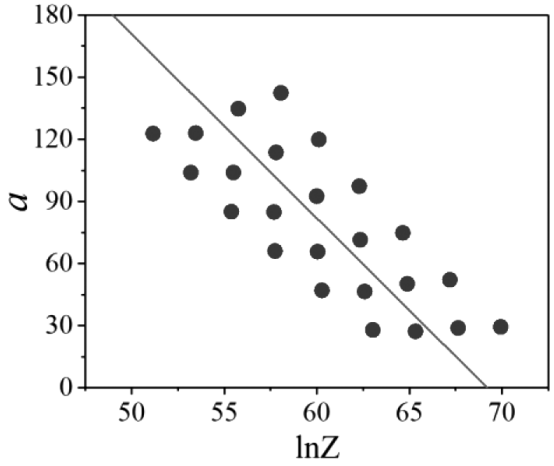

Figure 8: Relationship between a and lnZ

of strain on dynamic-recovery coefficient k_2 is added to the model to modify it.

Figure 7 shows the relationship between dynamic-recovery coefficient k_2 and strain when the strain rate is 1 s^{-1}. In accordance with the curve morphology in the figure, k_2 can be modified as follows:

$$k_2 = a \times 10^{b\varepsilon} + c \tag{33}$$

where a, b and c are the model coefficients.

The relationship between dynamic-recovery coefficient k_2 and strain can be fitted using the custom nonlinear function in the Origin software to obtain the model coefficients under different conditions. In accordance with the characteristics of the function from Equation (33) and through nonlinear fitting, coefficient b can be –6 and the value of coefficient c can be taken as the dynamic-recovery coefficient before the modification, namely $c = 228.0238\ Z^{-0.04496}$. Besides, the relationship

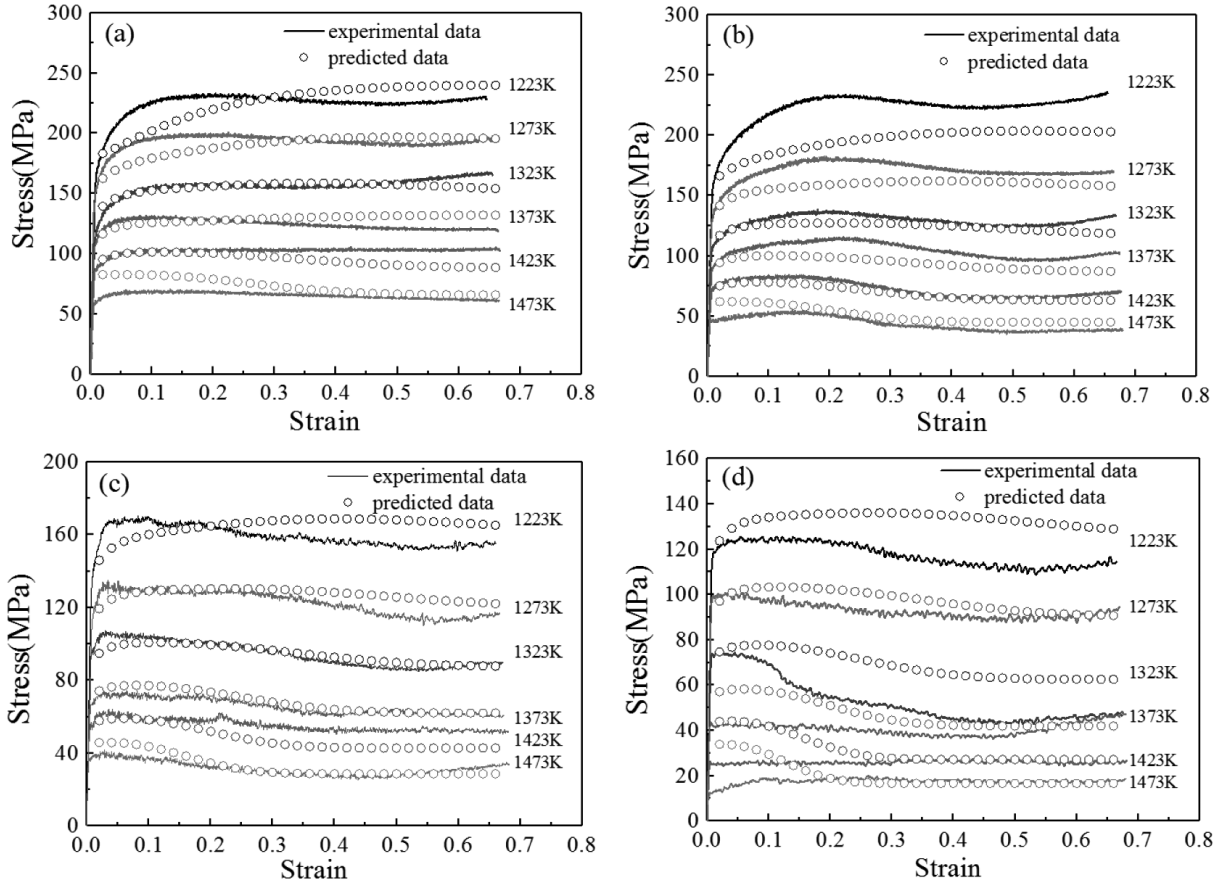

Figure 9: Comparison between the experimental and predicted flow stress at different strains for strain rates of: a) 1 s^{-1}, b) 0.1 s^{-1}, c) 0.01 s^{-1}, d) 0.001 s^{-1}

between coefficient a and ln Z is shown in **Figure 8**. Using linear fitting, it can be obtained that:

$$a = -8.90 \ln Z + 615.82 \tag{34}$$

In conclusion, the modified constitutive model for the as-cast Mn18Cr18N is:

$$\begin{cases} \sigma = \sigma_{rec}(\varepsilon < \varepsilon_c) \\ \sigma = \sigma_{drx}(\varepsilon \geq \varepsilon_c) \\ \sigma_{drx} = \sigma_{rec} - (\sigma_{sat} - \sigma_{ss})\left\{1 - \exp\left[-0.02324\left(\dfrac{\varepsilon - \varepsilon_c}{\varepsilon_p}\right)^{2.343}\right]\right\} \\ \sigma_{rec} = \sigma_{sat} - (\sigma_{sat} - \sigma_o)\exp(-k_2\varepsilon/2) \\ \sigma_{sat} = 0.998\sigma_p + 2.823 \\ \sigma_{ss} = 1.006\sigma_p - 14.720 \\ \sigma_0 = 0.681\sigma_p + 14.636 \\ \sigma_p = 108.11\sinh^{-1}(0.000152Z^{0.1478}) \\ k_2 = (-8.90\ln Z + 615.82)\times 10^{-6\varepsilon} + 228.0238Z^{-0.04496} \\ Z = \dot{\varepsilon}\exp(711073.274/RT) \\ \varepsilon_p = 1.11\times 10^{-4} Z^{0.10705} \\ \varepsilon_c = 0.88\times 10^{-5} Z^{0.10705} \end{cases} \tag{35}$$

Figure 9 shows graphs of comparisons between the modified constitutive model and experiments. The results show that the AARE is 10.2 % and the RMSE is 10.8 MPa. They show that the modified constitutive model can further reduce the error and improve the accuracy.

4 CONCLUSIONS

In this study, the thermal deformation behavior of the as-cast Mn18Cr18N steel was studied based on an isothermal-compression test involving deformation temperatures in a range of 1223–1473 K and strain rates in a range of 0.001–0.1 s^{-1}. Besides, a constitutive model for the steel at elevated temperatures was established. Based on these studies, the following conclusions were obtained:

1) The flow-stress curves of the as-cast Mn18Cr18N steel are of two types. One is the work hardening/dynamic recovery type and the other is the dynamic-recrystallization type. The dominant softening mechanisms of these two types of curves are dynamic recovery and dynamic recrystallization, respectively.

2) In accordance with the Arrhenius equation, the activation energy of the as-cast Mn18Cr18N steel is obtained and its value is 711073.274 J/mol.

3) Based on the traditional physically-based constitutive model, the dynamic-recovery coefficient of the model is revised and the influence of strain on the coefficient is considered in the modified model. Compared with the model before the modification, the prediction accuracy of the modified model is greatly improved. The AARE and RMSE are 10.2 % and 10.8 MPa, respectively.

Acknowledgments

The work was supported by the National Natural Science Foundation of China (No.51575372) and the Start-Up Fund for Scientific Research of the Taiyuan University of Science and Technology (No.20172011).

5 REFERENCES

[1] F. M.Qin, H. Zhu, Z. X. Wang, X. D. Zhao, W. W. He, H. Q. Chen, Dislocation and twinning mechanisms for dynamic recrystallization of as-cast Mn18Cr18N steel, Materials Science and Engineering: A, 684 (**2017**) 27, 634–644, doi:10.1016/j.msea.2016.12.095

[2] F. M. Qin, Y. J. Li, W. W. He, X. D. Zhao,H. Q. Chen, Effects of deformation microbands and twins on microstructure evolution of as-cast Mn18Cr18N austenitic stainless steel, Journal of Materials Research, 32 (**2017**) 20, 3864–3874, doi:10.1557/jmr.2017.389

[3] Z. H. Wang, H. P. Xue, W. T. Fu, Fracture Behavior of High-Nitrogen Austenitic Stainless Steel Under Continuous Cooling: Physical Simulation of Free-Surface Cracking of Heavy Forgings, Metallurgical & Materials Transactions A, 49 (**2018**) 5, 1470–1474, doi:10.1007/s11661-018-4561-z

[4] Y. C. Lin, J. Zhang, J. Zhong, Application of neural networks to predict the elevated temperature flow behavior of a low alloy steel, Computational Materials Science, 43 (**2008**) 4, 752–758, doi:10.1016/j.commatsci.2008.01.039

[5] Q. Yang, X. Wang, X. Li, Z. Deng, Z. Jia, Z. Zhang, G. Huang, Q. Liu, Hot deformation behavior and microstructure of AA2195 alloy under plane strain compression, Materials Characterization, 131 (**2017**) 500–507, doi:10.1016/j.matchar.2017.06.001

[6] J. H. Hollomon, Tensile Deformation, Transactions of the Metallurgical Society of AIME, 162 (**1945**), 268–290 (without doi)

[7] C. M. Sellars, W. J. McTegart, On the mechanism of hot deformation,ActaMetallurgica, 14 (**1966**) 9, 1136–1138, doi:10.1016/0001-6160(66)90207-0

[8] C. M. Sellars, Computer modeling of hot-working processes, Materials Science and Technology, 1 (**1985**) 4, 325–332, doi:10.1179/mst.1985.1.4.325

[9] B. S. Yu, S. L. Wang, T. Yang, Y. J. Fan, BP Neural Netwok Constitutive Model Based on Optimization with Genetic Algorithm for SMA,ActaMetallurgicaSinica, 53 (**2017**) 2, doi:10.11900/0412.1961.2016.00218

[10] L. Li, M. Q. Li, Constitutive model and optimal processing parameters of TC17 alloy with a transformed microstructure via kinetic analysis and processing maps, Materials Science & Engineering A, 698 (**2017**) 20, 302–312, doi:10.1016/j.msea.2017.05.034

[11] J. L. He, F. Chen, B. Wang, L. B. Zhu, A modified Johnson-Cook model for 10%Cr steel at elevated temperatures and a wide range of strain rates, Materials Science & Engineering, A, 715 (**2018**) 7, 1–9, doi:10.1016/j.msea.2017.10.037

[12] Y. C. Lin, X. M. Chen, D. X. Wen, M. S. Chen, A physically-based constitutive model for a typical nickel-based superalloy, Computational Materials Science, 83 (**2014**) 15, 282–289, doi:10.1016/j.commatsci.2013.11.003

[13] G. Z. Voyiadjis, A. H. Almasri, A physically based constitutive model for fcc metals with applications to dynamic hardness, Mechanics of Materials, 40 (**2008**) 6, 549–563, doi:10.1016/j.mechmat.2007.11.008

[14] F. Chen, X. D. Zhao, J. Y. Ren, H. Q. Chen, X. F. Zhang, Physically-Based Constitutive Modelling of As-Cast CL70 Steel for Hot Deformation, Metals and Materials International, (**2019**), doi:10.1007/s12540-019-00541-7

[15] C. Zener, J. H. Hollomon, Effect of Strain Rate Upon Plastic Flow of Steel, Journal of Applied Physics, 15 (**1944**) 1, 22–32, doi:10.1063/1.1707363

[16] Y. Estrin, H. Mecking, A unified phenomenological description of work hardening and creep based on one-parameter models, ActaMetallurgica, 32 (**1984**) 1, 57–70, doi:10.1016/0001-6160(84)90202-5

[17] H. Mecking, U. F. Kocks, Kinetics of flow and strain-hardening, ActaMetallurgica, 29 (**1981**) 11, 1865–1875, doi:10.1016/0001-6160(81)90112-7

[18] N. Hansen, D. Kuhlmann-Wilsdorf, Low energy dislocation structures due to unidirectional deformation at low temperatures, Materials Science and Engineering, 81 (**1986**) 141–161, doi:10.1016/0025-5416(86)90258-2

[19] Y. Estrin, Dislocation theory based constitutive modelling: foundations and applications, Journal of Materials Processing Technology, 80–81 (**1998**) 33–39, doi:10.1016/S0924-0136(98)00208-8

[20] H. M. Zhang, G. Chen, Q. Chen, F. Han, Z. D. Zhao, A physically-based constitutive modelling of a high strength aluminum alloy at hot working conditions, Journal of Alloys and Compounds, 743 (**2018**) 283–293, doi:10.1016/j.jallcom.2018.02.039